

Interaction of Cryogen Spray with Human Skin under Vacuum Pressures

Walfre Franco, Jie Liu & Guillermo Aguilar
*Department of Mechanical Engineering, University of California,
Riverside, USA.*

Abstract

Clinical results recently demonstrated improvement in lesion blanching using local vacuum to target small vessels in port wine stains (PWS) birthmarks laser therapy. The release of cryogen spurts under vacuum pressures may also offer many advantages to this therapeutic procedure due to different spray-surface interactions under vacuum conditions, which may lead to enhanced heat transfer. The objective of our work is to study the time and space dependent thermal response of a skin phantom to cryogen sprays at different pressures and constant humidity conditions. For this purpose, liquid cryogen was sprayed onto a skin phantom within atmospheric and various local vacuum pressures ranging from 17–70 kPa at 15 % and 50 % local humidity. We used a linear array of sensors mounted on the phantom surface to measure temperature changes as a function of time along a 6 mm radius, and a direct heat conduction solution to calculate the correspondent local heat fluxes. Compared to atmospheric pressures, lower minimum surface temperatures and higher heat fluxes from skin phantoms were observed along a 4 mm radius under all vacuum pressures and 15 % humidity. At 6 mm, there are no considerable differences in the heat transferred with or without vacuum application. At 50 %, the advantages of spraying in vacuum are less significant. Comparisons of results at constant pressures show that the heat extraction is more efficient at lower humidity levels. In general, the application of vacuum inherently reduces the content of water vapour. It follows that overall, the release of cryogen sprays under vacuum pressure enhances the heat extraction from the skin surface and, therefore, should help improve epidermal protection provided by cryogen spray cooling during PWS laser therapy.

Keywords: cryogen spray cooling, vacuum pressures, dermatologic surgery

1 Introduction

Clinical results of port wine stain (PWS) birthmarks laser therapy have shown that dark purple lesions usually respond well to the first 3–5 treatments. However, for most PWS, complete blanching is never achieved, and the lesion stabilizes at a red-pink colour. We have recently demonstrated that with the aid of a local vacuum applied to the lesion site prior to laser irradiation, photocoagulation of the smaller vessels in PWS birthmarks can be successfully achieved improving lesion removal [1]. We have then demonstrated that the release of cryogen spurts under vacuum pressures may also offer many advantages to this therapeutic procedure due to different spray-surface interactions under vacuum conditions: under hypobaric pressures, cryogen spurts did not produce skin indentation and only minimal frost formation; sprays also showed shorter jet lengths and better atomization; and, lower minimum surface temperatures and higher overall heat extraction from skin phantoms were reached by the centre of the sprayed surface [2]. In the latter study, as vacuum was applied the local humidity level changed; that is, the reported changes are due to a combined reduction in pressure and humidity. In the present study the objective is to assess the effect of pressure variations with time and the radial dependent heat transferred during cryogen spray cooling of a skin phantom. To this end, we use a linear array of sensors, maintain the level of water vapour constant and release cryogen spurts at different pressure conditions onto a skin phantom enclosed in an experimental chamber.

2 Materials and Methods

2.1 Spray system

Refrigerant R-134a (Suva® 134a, Dupont, Wilmington DE), with a boiling temperature $T_b \approx -26.2$ °C at atmospheric pressure, was delivered from its original container (at 600 KPa and 22 °C) to a fuel injector attached to a stainless steel straight-tube nozzle—with 0.7 mm inner diameter and 32 mm length. The spray system was set to deliver single 60 ms spurts 30 mm away from the phantom surface.

2.2 Thermal sensor and skin model

The thermal sensor used four type-K thermocouples (CHAL-005, Omega, Stamford, CT, USA) soldered to a linear array of four silver discs (S1, S2, S3 and S4) embedded in an epoxy resin (RBC 3100, RBC, Warwick RI), see Fig. 1. The diameter and thickness of each disc were 1 and 0.09 mm, respectively, and the separation between discs was 1 mm. The sensor employed, similar to those reported previously [3], provided a substrate with thermal properties similar to human skin. The standard error limit of type-K thermocouples is 2.2 °C or 2%. Specific heat c , density ρ , thermal conductivity k and thermal diffusivity α of epidermis, epoxy and silver foil are presented in Table 1. Temperature was

acquired through instruNet hardware (GW Instruments, Inc., Somerville, MA, USA) and National Instruments software (LabView 7) at 800 Hz. Noise was filtered out using a running average of previous and next 10 points. The initial temperature of the thermal sensor before any spurt was 22 °C for all experiments.

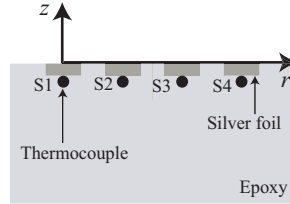


Figure 1: Thermal sensor and skin model

Table 1: Thermal properties

	epidermis	epoxy	silver foil
c (J/kg K)	3600	—	235
ρ (kg/m ³)	1200	1160-1400	10500
k (W/m K)	0.21	0.217	429
α (m ² /s)	0.5×10^{-7}	1.2×10^{-7}	1739×10^{-7}

Table 2: R-134a saturation temperatures

P (kPa) [in Hg]	P_{abs} (kPa)	$\approx T_{sat}$ (°C)
0	101.3	-26
16.9 [5]	84.4	-30
33.9 [10]	67.4	-35
50.8 [15]	50.5	-40
67.7 [20]	33.6	-48

2.3 Vacuum pressure chamber

A 300×380 mm cylindrical vacuum chamber (Terra Universal Inc., Anaheim CA) made of acrylic was used to enclose the spray system, thermal sensor and skin phantom. The chamber pressure was lowered by a vacuum pump to carry out experiments at 0, 16.9, 33.9, 50.8 and 67.7 kPa (0, 5, 10, 15 and 20 in Hg) vacuum pressures (relative to the atmospheric pressure) at a constant 15 % humidity, and at 0 and 50.8 kPa (0 and 15 in Hg) vacuum pressures at 50 % humidity. Relative humidity was controlled by flushing the chamber with an air-nitrogen gas mixture. Saturation temperatures of liquid cryogen at these pressures are shown in Table 2.

2.4 Heat transfer calculations

Temperatures recorded by our thermal sensor are assumed to be surface temperatures since the silver disc Biot (hL/k) number for a heat transfer coefficient $h = 20\,000$ W/m²K [4] is ≈ 0.004 . Duhamel's theorem states that the

substrate thermal response at t equals the total sum of what the substrate experienced in small steps prior to t . Assuming constant thermal properties, Duhamel's theorem can be written as

$$\theta(z, t) = \theta_o + \int_{t_o}^t u(z, t - \tau) \frac{dT}{d\tau} d\tau, \quad (1)$$

where z is the coordinate perpendicular to the surface, T is the surface temperature, θ is the substrate temperature, θ_o is the uniform initial temperature, u is the temperature response function of the substrate (initially at zero temperature) to a unit step in surface temperature, and $t - \tau$ is the time that has elapsed since the step at τ . The unit step function for a semi-infinite planar solid is

$$u(z, t) = 1 - \operatorname{erf}\left(\frac{z}{2\sqrt{\alpha t}}\right). \quad (2)$$

Substituting Eqn. 1 and 2 into Fourier's law gives

$$q(t) = \sqrt{\frac{k\rho c}{\pi}} \int_{t_o}^t \frac{1}{\sqrt{t - \tau}} \frac{dT}{d\tau} d\tau, \quad (3)$$

which can be integrated analytically to calculate the approximate surface heat flux q' in a semi-infinite planar body with discrete surface temperature measurements T_i at time t_i as

$$q'(t_I) = 2\sqrt{\frac{k\rho c}{\pi}} \sum_{i=1}^I \frac{T_i - T_{i-1}}{\sqrt{t_I - t_i} + \sqrt{t_I - t_{i-1}}}. \quad (4)$$

Equation 4 was used to calculate the surface heat flux. For simplicity, q' is written as q in the next sections. A more detailed derivation of Eqn. 4 can be found in [5].

3 Results and Discussion

The linear array of sensors S1, S2, S3 and S4 was aligned respect to the centre of the sprayed surface such that the discs centres were respectively at $r = 0, 2, 4$ and 6 mm. At atmospheric conditions, the diameter of the fully developed spray cone was ≈ 8 mm and the maximum diameter of the sprayed surface was ≈ 20 mm.

3.1 Pressure effects at 15 % humidity

Results presented in this subsection correspond to five different pressure conditions at 15 % relative humidity; we used this set point because at our facility, normally at 30–40 % atmospheric humidity, a 50.8–67.7 kPa (15–20 in Hg) reduction in the pressure chamber yielded 15 % humidity (without flushing with an air-nitrogen gas mixture).

3.1.1 Surface temperature and heat flux dynamics

Temporal changes in surface temperature T and heat flux q at each radial location for two pressure conditions are shown in Fig. 2. Solid lines correspond to atmospheric pressure and discontinuous lines to 50.8 kPa (15 in Hg). Although we carried out experiments at various pressures, this study compares these two pressures because 50.8 kPa seems to be the highest suction pressure that may be used without inflicting discomfort to patients. Figure 2a shows that the difference in T with and without vacuum was not significant during the first 60 ms (pulse width duration). Quantitative and qualitative differences began at ≈ 80 ms which corresponds to the end of in-flight liquid cryogen due to opening and closing delays (mainly because of the valve mechanics) of approximately 8 and 10 ms. In general, at S1 and S2 (0 and 2 mm) T was equal or lower using vacuum to that at atmospheric pressure. At S3 (4 mm) T was lower using vacuum even before spurt termination, which may have happened because the spray cone widened as the pressure was decreased covering completely the sensor at vacuum pressure—as mentioned, 4 mm corresponds to the spray cone edge at atmospheric conditions. At S4 (6 mm), cooling took place mainly because of the liquid film flow established at the surface during cryogen spread; herein T was slightly lower at atmospheric pressure.

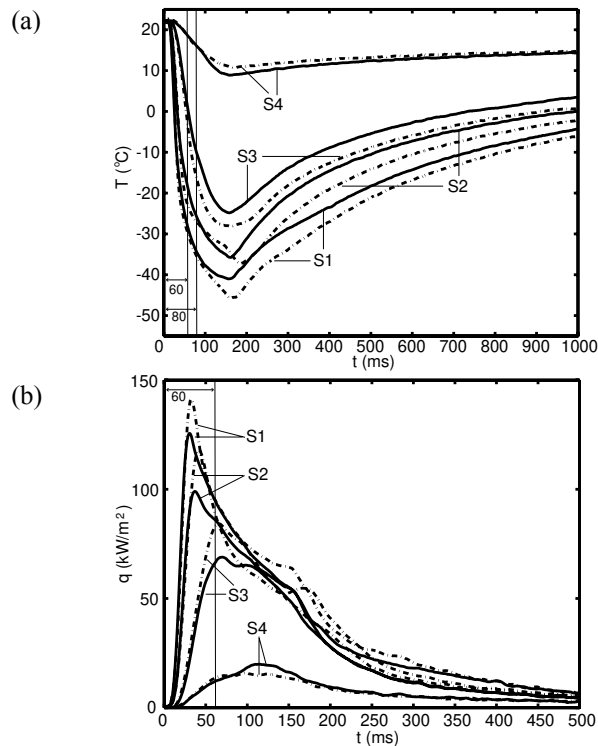


Figure 2: (a) Surface temperature and (b) heat flux at — atmospheric and - - - 50.8 kPa (15 in Hg) vacuum pressures; 15 % relative humidity

Figure 2b shows that in general q was larger at vacuum pressure in S1, S2 and S3 (0, 2 and 4 mm) but slightly lower in S4 (6 mm). Note that whether atmospheric or vacuum conditions exist, the maximum q at each location occurred at different times: the closer to the centre of the sprayed surface the faster it occurred. Note also that the qualitative characteristics of each curve change from the centre of the sprayed surface to the periphery. It follows that the thermodynamics of spray-skin phantom interactions are pressure, time and space dependent—a consequence of the complexity of evaporating sprays. For instance, it is possible that liquid cryogen accumulated on the surface creating a pool that shrank towards the centre of the spray since the boiling temperature of cryogen at atmospheric conditions is ≈ -26 °C (Table 2) and T at S1 and S2 decreased and remained below this temperature. The boiling temperature of cryogen at 50.8 kPa of vacuum pressure is ≈ -40 °C (Table 2) and T was below this temperature only at S1; it follows that a smaller pool of liquid cryogen may have taken place.

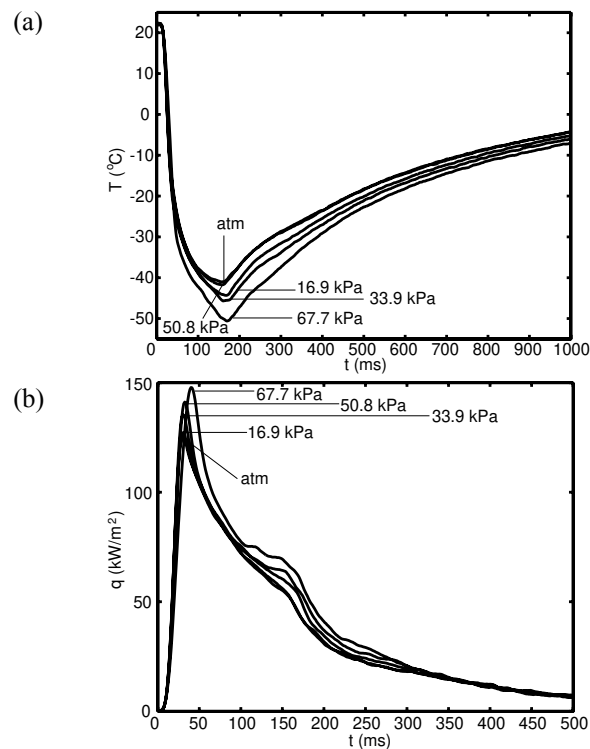


Figure 3: (a) Surface temperature and (b) heat flux at atmospheric and 16.9, 33.9, 50.8 and 67.7 kPa (0, 5, 10, 15 and 20 in Hg) vacuum pressures; 15 % relative humidity.

Figure 3 shows dynamics of T and q at the centre of the sprayed surface (S1) for atmospheric and 16.9, 33.9, 50.8 and 67.7 kPa (0, 5, 10, 15 and 20 in Hg) vacuum pressures. At the centre of the sprayed surface, as the pressure decreased a lower T was reached at the skin phantom and a higher q establishes between the skin phantom, spray and surroundings.

3.1.2 Minimum surface temperatures and maximum surface heat fluxes

The surface temperature minima T_{min} and heat flux maxima q_{max} reached at each location are shown in Fig. 4 as a function of pressure and constant 15 % humidity. In Fig. 4a, a lower T_{min} was reached at S1, S2 and S3 (0, 2 and 4 mm) as the pressure decreased while at S4 the vacuum pressure effect on the heat transferred seems to be small.

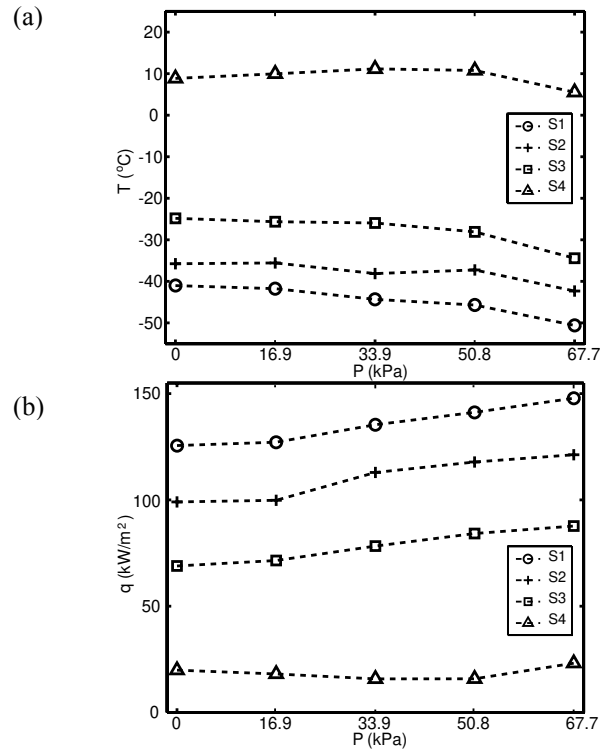


Figure 4: (a) Minimum surface temperatures and (b) maximum surface heat fluxes.

The enhanced heat extraction measured in these experiments is a consequence of the effect that vacuum pressures have on the atomization and evaporation dynamics of cryogen spray droplets; by lowering the discharge pressure the liquid cryogen goes through larger expansions that increase its exit velocity. Consequently, the cryogen experiences larger shear stresses that enhance atomization and accelerate evaporation.

3.2 Pressure effects at 50 % humidity

Temporal changes in surface temperature T and heat flux q at each radial location for two pressure conditions at 50 % relative humidity are shown in Fig. 5. Solid lines correspond to atmospheric pressure and discontinuous lines to 50.8 kPa (15 in Hg). In Fig. 5a, lower temperatures were reached at S1 and S2 using vacuum while lower temperatures were reached at S3 and S4 at atmospheric pressure. In Fig. 5b, a higher heat flux established at S1 at atmospheric pressure from 0–150 ms, for $t > 150$ ms q was higher at vacuum pressure. At S2 with vacuum, q is higher or similar to that at atmospheric pressure. At S3 and S4 q was higher at atmospheric conditions. By comparing areas under the curves in Fig. 5b, we see that overall the heat transfer at S1 and S2 was more efficient at 50.8 kPa because larger amounts of heat were removed; that is, values of the time integral (from 0 to 500 ms) of the correspondent $q(t)$ in Fig. 5b are larger than those at atmospheric pressure. As mentioned, lower pressures enhance atomization and evaporation benefiting the heat transfer at low humidity, as shown in Fig. 4. At high humidity a better atomization and evaporation may translate in faster condensation and larger amounts of condensed water vapour which, as explained below, inhibits the heat extraction from the skin phantom.

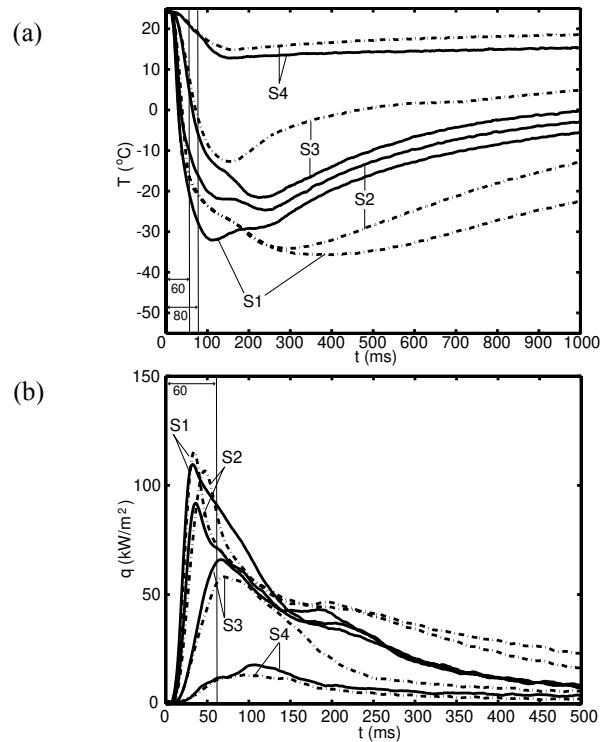


Figure 5: (a) Surface temperature and (b) heat flux at — atmospheric and - - - 50.8 kPa (15 in Hg) vacuum pressures; 50 % relative humidity.

The effects of relative humidity on the spray-skin phantom heat transfer interactions can be seen by comparing Figs. 2 and 5. Overall, the humidity was detrimental for the heat extraction process [6]: as the humidity increased, lower T and q were reached at every radial location. Comparing the curves of S1 and S2 at vacuum conditions in Figs. 2b and 5b, at $t = 500$ ms $q < 10$ kW/m² at 15 % of humidity while $q \approx 20$ kW/m² at 50 %; that is, cooling was prolonged by the centre of the sprayed surface at high humidity. A similar situation is seen by comparing S1 and S2 curves at atmospheric conditions. Reduced and extended heat fluxes are a consequence of water vapour condensation, which becomes a heat sink building a thin layer of ice that remains after spurt termination.

The enhanced heat extraction measured in these experiments is a consequence of the effect that vacuum pressures have on the atomization and evaporation dynamics of cryogen spray droplets, which may be observed as variations in the spray droplet size, velocity and temperature distributions with respect to those at atmospheric pressure. Our ongoing work is focused on establishing the relationship between these spray property variations and the overall heat extraction resulting from spraying cryogen sprays under vacuum pressures.

4 Conclusions

This study focused on measuring the overall effect of vacuum pressures on the heat extraction from human skin phantoms along a 6 mm radius during cryogen spray cooling (CSC). Lower surface temperatures and higher surface heat fluxes with respect to atmospheric conditions take place at 15 % humidity along a 4 mm radius. At 6 mm, there are no considerable differences in the heat transfer. Experiments at 50 % local humidity show that the advantages of using vacuum are not as significant. Comparisons of results at constant pressure show that the heat extraction is more efficient at lower humidity levels. In general, the application of vacuum inherently reduces the content of water vapour, i.e., humidity level. Therefore, on the whole, CSC under vacuum pressures enhances the heat extraction from the skin surface compared to that measured at atmospheric pressure. These results alone should help improving epidermal protection provided by CSC during PWS laser therapy.

5 Acknowledgements

This work was supported in part by the National Institutes of Health (HD42057), the Regents of the University of California Riverside Faculty Fellowship and the A. Ward Ford Research Grant from the American Society of Lasers in Medicine and Surgery.

6 References

1. Aguilar, G., Svaasand, L.O., and Nelson, J.S., *Enhancement of purpura through the use of local vacuum*. Lasers in Surgery and Medicine, 2004: p. 4-4.
2. Aguilar, G., Franco, W., Liu, J., and Nelson, J.S., *Effects of hypobaric pressure on human skin: implications for cryogen spray cooling (part II)*. Lasers in Surgery and Medicine, 2005.
3. Basinger, B., Aguilar, G., and Nelson, J.S., *Effect of skin indentation on heat transfer during cryogen spray cooling*. Lasers in Surgery and Medicine, 2004. **34**(2): p. 155-163.
4. Jia, W.C., Aguilar, G., Wang, G.X., and Nelson, J.S., *Heat-transfer dynamics during cryogen spray cooling of substrate at different initial temperatures*. Physics in Medicine and Biology, 2004. **49**(23): p. 5295-5308.
5. Franco, W., Liu, J., Wang, G.X., Nelson, J.S., and Aguilar, G., *Radial and temporal variations in surface heat transfer during cryogen spray cooling*. Physics in Medicine and Biology, 2005. **50**(2): p. 387--397.
6. Majaron, B., Kimel, S., Verkruysse, W., Aguilar, G., Pope, R., Svaasand, L.O., Lavernia, E.J., and Nelson, J.S., *Cryogen spray cooling in laser dermatology: Effects of ambient humidity and frost formation*. Lasers in Surgery and Medicine, 2001. **28**(5): p. 469-476.